A study of Cardiopulmonary interaction haemodynamics with detailed lumped parameter model

K. Hemalatha and M. Manivannan*

Biomedical Engineering Laboratory,
Department of Applied Mechanics,
Indian Institute of Technology Madras,
Chennai 600036, Tamil Nadu, India
Fax: +91-44-2257 4652
E-mail: hemaa75@gmail.com
E-mail: mani@iitm.ac.in
*Corresponding author

Abstract: A Cardiopulmonary (CP) model to study the interaction between Cardiovascular(CV) and Respiratory System (RPS) is presented. It includes detailed anatomical representations of CV, RPS and baroreflex control. The respiratory induced variations on CVS is realized by intrapleural pressure (Ppl). The state equations are solved using 4th order Runge-Kutta method. Sensitivity analysis is performed. The RPS influences on aortic pressure is presented for quite breathing and Valsalva Manuever and found have good agreement with literature data. Our model can simulate various CP diseases and therefore it can be used to study interactions hemodynamics in normal and pathological conditions.

Keywords: haemodynamics; lung mechanics; gas exchange; baroreflex; intrapleural pressure; septum.

Reference to this paper should be made as follows: Hemalatha, K. and Manivannan, M. (xxxx) 'A study of Cardiopulmonary interaction haemodynamics with detailed lumped parameter model', *Int. J. Biomedical Engineering and Technology*, Vol. x, No. x, pp.xxx–xxx.

Biographical notes: K. Hemalatha received her Master's Degree in Biomedical Engineering from Indian Institute of Technology Madras in 2004. Currently, she is a Doctoral Student at Biomedical Engineering Laboratory, Department of Applied Mechanics, Indian Institute of Technology Madras, Chennai, India. Her research interests are in the areas of mathematical modelling, instrumentation and signal processing.

M. Manivannan received his PhD and Master's Degree in Mechanical Engineering from Indian Institute of Science Bangalore, India, in 2000 and 1992, respectively. Currently, he is a Faculty in Biomedical Engineering, Department of Applied Mechanics, Indian Institute of Technology Madras, Chennai, India. His research interests are in the areas of haptics, quantitative physiology and medical simulations.

1 Introduction

Cardiopulmonary (CP) diseases need better understanding of their interactions for diagnosis and treatment (Rustagi, 1971). Mathematical models can provide more information regarding both invasive and noninvasive parameters related to Cardiovascular System (CVS) and Respiratory System (RPS). Our objective is to develop a detailed model of CP with the facility of simulating all kinds of diseases related to CVS and RPS and their influence on each other. This model integrates three distinct models, heart with closed-loop circulation reported by Sun et al. (1997), respiratory system with lung mechanics developed by Athanasiades et al. (2000) and gas exchange model developed by Liu et al. (1998). A comprehensive survey of mathematical models to study the interaction of CV and respiratory system varies significantly in their complexity, assumptions and objectives (Chung et al., 1997; Mukkamala and Cohen, 2001; Luo et al., 2007). Many authors have constructed separate models to explain CV system behaviour in normal as well as pathophysiological conditions (Burkhoff and Tyberg, 1993; Hay et al., 2005; Jung and Lee, 2006) and respiratory systems (Jackson and Milhorn, 1973; Anderson et al., 2009). The interaction between CV and respiratory model is incorporated in many models only by modulating intrathoracic pressure in terms of respiratory frequency as reported by Beyar et al. (1987) and Cherniack and Longobardo (2006) without coupling detailed respiratory model. A comprehensive CP model with detailed circulatory model, lung mechanics and gas exchange has been reported in Lu et al. (2001). However, in their model, the turbulent flow nature of cardiac valves, time varying viscoelastic property of pulmonary circulatory, and parameter simulate valvular disease were not addressed. Our model includes

1 CV model of four cardiac chambers with proportional valves, pulmonary and systemic circulation, pericardium, septum and baroreflex control
2 Respiratory model with lung mechanics and gas exchange.

Our model, therefore, has the advantages of simulating normal and pathological conditions of CVS and RPS and also their interaction in the above-mentioned conditions.

2 Model formulation

2.1 Cardiovascular model

The general form of the CV model is based on the work of Sun et al. (1997). With the focus of our objective, the base has been modified. The following simplifications are made on the base model.

The after-load systemic circulation is simplified with aorta, artery and capillary, coronary circulation is removed, systemic circulation compliances are modelled with simple capacitances and cosine activation function is used for cardiac chamber elastance.

Figure 1 shows the electrical analogue of CV model.

Figure 1 Cardiovascular system model

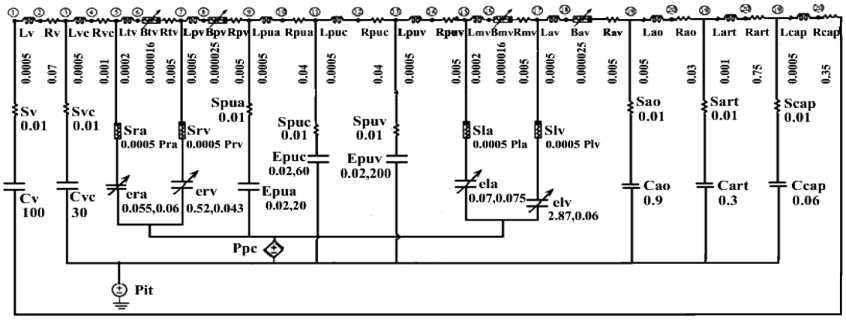

2.1.1 Heart model

Heart model includes four cardiac chambers with four heart valves. Left and ventricles can be modelled as three-walled system; Right Ventricle (RV) free wall, Left Ventricle (LV) free wall, and septal coupling wall (Olansen et al., 2000). The viscoelastic property of the heart chamber free walls is modelled with time-varying elastance according to a cosine charging and discharging function. The LV free wall elastance is formulated as follows

$$e_{lv} = \begin{cases} F_L . E_{lva} . 0.5 . \left(1 - \cos\left(\dfrac{\pi t}{t_{ee}}\right) + \dfrac{E_{lvb}}{F_L}\right) & t \le t_{ee} \\ F_L . E_{lva} . 0.5 . \left(1 + \cos\left(\dfrac{\pi (t - t_{ee})}{0.5 t_{ee}}\right) + \dfrac{E_{lvb}}{F_L}\right) & t \le 1.5 t_{ee} \\ \dfrac{E_{lvb}}{F_L} & \text{otherwise} \end{cases} \tag{1}$$

where e_{lv} [mmHg · ml^{-1}] represent the time-varying elastance of the LV free wall, t_{ee} is the [0.3 s] end ejection time and e_{lv} repeats the same pattern of changes for every cardiac cycle (0.855 s). F_L is a scaling factor that characterises the non-linear property of the starling law and the dependence of the time-variant elastance on the volume of the LV.

$$F_L = 1 - \left(v_{lv} \Big/ v_{\max}\right) \tag{2}$$

where $v_{\max}$ is the maximum cardiac fluid volume of normal human (900 ml). In similar way, right ventricle elastance can also be written. The corresponding parameter values are given in Figure 1. The coupling septal wall offers direct pressure coupling between left and right ventricles through its constant elastance (E_s). Hence, the functional elastance of both ventricles are given as

$$e_{lvf} = E_s \,.\, e_{lv} \Big/ \left(e_{lv} + E_s\right) \tag{3}$$

$$e_{\text{rvf}} = E_s \,.\, e_{rv} \Big/ \left(e_{rv} + E_s\right) \tag{4}$$

Because of the pressure coupling realised by the septum between two ventricles, the net pressure of each ventricle is given as,

$$p_{lv} = e_{\text{lvf}} \,.\, v_{lv} + \frac{e_{lv}}{\left(e_{lv} + E_s\right)} p_{lv} \tag{5}$$

Similar way, right ventricle pressure can also be formulated. The atrium septum is assumed to be rigid so that both atriums are uncoupled and have no direct influence on each other. So, the free walls of the atriums are characterised by a time-varying elastance as follows.

For Left Atrium (LA)

$$e_{la} = \begin{cases} E_{\text{laa}} \,.\, 0.5\left(1 - \cos\left(\pi\left(t - t_{ac}\right) \Big/ \tau_{\text{lac}}\right)\right) + E_{\text{lab}} & t_{ac} \le t \le t_{ar} \\ E_{\text{laa}} \,.\, 0.5\left(1 + \cos\left(\pi\left(t - t_{ac}\right) \Big/ \tau_{\text{lar}}\right)\right) + E_{\text{lab}} & t_{ar} \le t \le \left(t_r + t_{ac}\right) \\ E_{\text{lab}} & \text{otherwise} \end{cases} \tag{6}$$

where e_{la} [mmHg · ml^{-1}] represent the elastance of the Atrium, t_r [0.855 s] indicate a cardiac cycle, t_{ac} [0.696 s] refers to the time when the atrium begins to contract and t_{ar} [0.835 s] indicates the time when the atrium begins to relax. RA elastance can be formulated as LV by appropriately replacing LV parameters.

2.1.2 Heart valves

The heart valves non-linear time-dependent behaviour is addressed by modelling them with three elements based on Sun et al. (1995). They are

1 Bernoulli's resistance (S), (relates pressure-flow relation at the orifice based on Bernoulli's principle)

2 Inertance (L) (relates the acceleration and deceleration of flow)

3 Viscous resistance (R).

The opening of the valves is due to forward pressure difference between two anatomical locations Separated by them (for mitral valve $p_{la} > p_{lv}$).

2.1.3 Systemic and pulmonary circulation

The systemic circulation is modelled with simple capacitance where as an exponential P-V relationship is adopted for pulmonary circulation to achieve effective coupling between respiratory and CV systems. The P-V relationship is given as follows

$$p = E_0 \left(e^{V/Z} \right) Z \tag{7}$$

where E_0 (mmHg · ml^{-1}) denotes the zero-volume elastance, Z (ml) refers to the volume constant and v [ml] is the volume of the corresponding pulmonary circulatory unit (artery/vein).

2.1.4 Pericardium

The volume coupling is offered by the pericardium among all chambers in the pericardial cavity as reported by Hoit et al. (1993). It gives significant constrain on the filling capabilities of the heart chambers. So, the total cardiac fluid volume includes blood volume and pericardial fluid volume (v_{pe} = 30 ml).

$$V_{pc} = v_{ra} + v_{rv} + v_{la} + v_{lv} + v_{pe}. \tag{8}$$

The pericardial pressure has exponential relationship with volume and is given by

$$p_{pc} = \mathrm{e}^{\frac{v_{pc} - v_{pc0}}{v_{\mathrm{con}}}} \tag{9}$$

where V_{pc0} is the zero-volume constant of pericardium and V_{con} is the volume constant of pericardium.

2.1.5 Baroreflex control

Arterial pressure regulation (Shahin and Maka, 2007) is considered to represent controlled heart model. Therefore, baroreflex is modelled by controlling heart rate based on systolic peak pressure of aorta (P_{aos}), which is given as follows.

$$HR = K_{\mathrm{baro}} \Big/ \left(P_{\mathrm{aos}} - 120 \right) + HR_0 \tag{10}$$

where K_{baro} is 188.68 based on De Boer et al. (1987) and HR_0 is 70 beats/min.

2.2 Respiratory model

The respiratory model consists of lung mechanics model based on Athanasiades et al. (2000) and gas exchange model based on Liu et al. (1998) and Lu et al. (2001) with some modifications (Figure 2). In general, gas transport occurs at two sites; between alveoli air and pulmonary capillary blood, between systemic capillary blood and cellular fluid. Our gas exchange model is limited to characterise gas transport only between blood and air at alveoli (lung gas exchange) not at tissue level (between blood and cellular fluid).

Figure 2 Respiratory system model

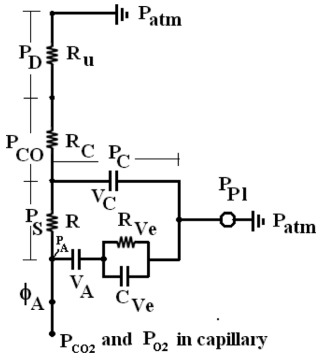

2.2.1 Lung mechanics

In our lung mechanics model, airway of the respiratory system is subdivided as small airway (alveolar region), collapsible airway and upper airway. Alveolar region is lumped as a single unit and termed as small airway. It (of volume V_A) is assumed to exhibit non-linear behaviour and the time-varying viscoelastic behaviour of lung tissue (Fredberg and Stamenovic, 1989; Jonson et al., 1993) is modelled by two-element Kelvin body, which incorporates capacitance to represent elastic nature and resistance to viscous dissipative property. The small air way is characterised by a resistor (Rs), which is exponentially related to alveolar volume (V_A) and residual volume (RV) as reported in Golden et al. (1973) and Olender et al. (1976).

$$Rs = A_s(\mathrm{e}^{Ks(VA-RV)} / V^* - RV) \tag{11}$$

where V^* is the maximum alveolar volume at the end of inspiration and A_s is the scaling parameter. In quite breathing, inhalation is an active process where as the exhalation is a passive process. So, the collapsible airway resistance Rc has different values for the two respiratory phases. The value for Rc during expiration is greater than that during inspiration and is characterised in terms of a non-linear volume-dependent resistance based on Golden et al. (1973).

$$Rc = \begin{cases} Kco & Vc > Vc\max \\ Kco\left(\dfrac{Vc\max}{Vc}\right)^2 & Vc \le Vc\max \end{cases}. \tag{12}$$

The upper airway (dead space region) is also modelled by a non-linear, volume-dependent resistance.

$$Ru = Au + Ku\,|Vcw| \tag{13}$$

where Au is the offset and Ku is the scaling factor. The lung and airways are assumed to be enclosed within a rigid-walled thoracic cage, with the airways open to the atmosphere. The spatially averaged time-varying intrapleural pressure is driving the respiratory model. Excursion in pleural pressure is dictated by the effort generated by the subject. So, the source for the respiratory model is the time-varying intrapleural pressure. Based on mass conservation principle, volume state equation (1st order differential equation) for the

two compliant compartments of RPS are formulated. The coupling between lung mechanics and gas exchange are achieved by including gaseous alveolar flux flow in lung mechanics (Appendix).

2.2.2 Gas exchange model

Gas exchange between blood and air occurs across the alveolar–capillary membrane. The following assumptions are made in our model:

1 inspired air is instantaneously warmed to body temperature (300 K) and fully saturated with water vapour

2 the gaseous mixture obeys the ideal gas law

3 blood is considered as a uniform homogeneous medium (plasma and erythrocytes are lumped together)

4 within a control volume, the instantaneous specific reactions are considered to be at equilibrium

5 diffusion in radial and axial directions are not considered as in Lin and Cumming (1973), so bulk gas transport occurs only in axial direction

6 diffusion is the sole cause of gas transport (Lu et al., 2003) and its rate depends on lung diffusion capacity (D_L) for the particular species (O_2 and CO_2)

7 one-directional diffusion is assumed (O_2 from air to blood and CO_2 from blood to air)

8 N_2 diffusion is neglected, which has either way diffusion

9 35 capillary segments and 35 alveolar units reported in Lu et al. (2001) are lumped as single capillary and single alveolar unit.

Based on ideal gas law, the partial pressure of O_2 and CO_2 in all airways and in systemic, pulmonary circulation are written (Appendix).

2.2.3 P_{pl}-mediated CP interaction

The interactions between CV and respiratory system could be incorporated in a variety of forms. In general, to study the interaction between two subsystems, generally one subsystem is perturbed and the other subsystem parameters are monitored. In our model, the driving pressure of the respiratory system (P_{pl}) is perturbed and the aortic pressure pulse of CV system is monitored. To influences of RPS on CVS is simulated by incorporating the pleural pressure variations in the CV system directly to all compartments that lie in the thorax, which include vena cava, right heart, pulmonary circulation, left heart and aorta (Sun et al., 1997; Lu et al., 2001).

3 Results and discussion

3.1 Numerical methods and parameters

In CV model, elastance or capacitance nodes are considered for formulating volume equations according to mass balance principles and flow equations are formulated for inertance nodes based on continuity equations. Similar way, respiratory, volume (elastance or capacitance) and flow equations (through airway resistances) are written. The partial pressure equations of O_2 and CO_2 in blood and air are formulated based on ideal gas law. The state equations are given in Appendix.

Fourth-order Runge-Kutta numerical method is used to solve the state equation for a time step of 10 ms. The model-based simulation software is written completely using MATLAB 7.4 (R2007a). Two-step model parameter identification procedure is adopted. Initially, they are roughly taken from physiological ranges reported in literature based on experimental works and then fine-tuned to yield accurate haemodynamic waveforms. The tuned model parameters of CV system are shown in Figure 1 and respiratory parameters are given in Table 1.

Table 1 Model parameters for respiratory system

Parameter	*Value*	*Parameter*	*Value*
K_{co}	1.54×10^{-4} mmHg · ml^{-1} s^{-1}	K_{cytox}	1.00E-9 mol/ml
A_s	1.6×10^{-3} mmHg/ml/s	K_1	0.001
A_u	2.5×10^{-4} mmHg/ml/s	nH	2.3
Bc	27.43 mmHg	$P50_{O2}$	26.5 mmHg
B_{cp}	2.74 mmHg	P_{ao}	760 mmHg
B_1	0.368 mmHg	P_{mouth}	0 mmHg
C_{ve}	680 ml/mmHg	P_s	166.67 ml/s
K_{co}	1.54×10^{-4} mmHg/ml/s	P_{STP}	760 mmHg
K_1	0.001	R_{paoCO2}	0.0003
K_s	–10.9	R_{paoO2}	2.10E-01
K_u	3.3×10^{-7} mmHg/ml/s^2	RQ	0.8
RV	1650 ml	T_{body}	300 K
Rco	0 mmHg	T_{stp}	273 K
R_{ve}	7.3×10^{-4} mmHg/ml/s^2	B_{wt}	60 Kg
α_{CO2}	3.26E-08 mol/ml/mmHg	V^*	5300 ml
α_{O2}	1.36E-06 mol/ml/mmHg	V_{cmax}	185 ml
CHb	2×10^{-5} mol/ml	V_{cytox}	0.21 mol/sec/kg
H_{crit}	0.45	V_{isf}	48000 ml

3.2 Sensitivity analysis

The sensitivity of each parameter of the CV model to important haemodynamic parameters has been analysed. The sensitivity is quantified by computing a gain factor, which is the ratio of percent change of affected haemodynamic parameter and percent

change of affecting model parameter. Each model parameter is perturbed by a 10% increase from its control value. The simulation is run for few cardiac cycles (10 cycles) to settle from initial transients. From the settled response, the sensitivity gain is calculated for each parameter. The parameter for which the sensitivity gain ≥ 0.1 is considered and tabulated in Table 2, the remaining parameters are considered as insensitive, which are not given in the table. Systemic after-load resistance R_a and aortic valve resistance (R_{av}) and Venous compliances (C_{ven}) are sensitive because they are the major determinants of cardiac output and aortic pressure. All haemodynamics are more sensitive to ventricular elastance, which represents the pumping action of heart in CV system. Intrapleural pressure (P_{pl}) has good sensitivity; this may be due to its direct influence on cardiac units that lie inside the intra thoracic cavity. The qualitative sensitivity analysis of respiratory system can be done by changing the functional description of resistances and compliances, which is well explored in Liu et al. (1998).

Table 2 Sensitivity analysis in terms of gain for CV model simulation

	HR	V_{lv}	V_{pua}	V_{vc}	*MAP*	P_{lv}
R_{art}	–0.1	–0.1	0.1	0.1	0.1	0.2
E_{puv0}	NS	–0.1	0.3	0.1	0.1	0.4
E_{pua0}	–0.1	NS	–0.3	0.1	NS	0.1
E_{raa}	NS	NS	NS	NS	0.1	NS
E_{rab}	NS	NS	0.1	NS	0.1	0.1
E_{rva}	–0.1	NS	NS	NS	0.1	0.2
E_{rvb}	–0.1	0.1	0.2	NS	NS	–0.2
E_{laa}	0.1	0.1	0.1	NS	NS	–0.1
E_{lab}	NS	NS	0.1	NS	0.1	0.1
E_{lva}	–0.1	NS	0.2	0.1	0.2	–0.2
E_{lvb}	–0.2	–0.2	0.2	0.1	0.2	0.5
V_{pco}	–0.2	0.1	0.1	NS	0.2	0.1
P_{pl}	–0.3	0.1	0.1	NS	0.2	0.3
C_{vc}	0.1	NS	NS	NS	NS	NS
C_{art}	0.1	NS	–0.1	NS	–0.1	0.1

NS: Not Sensitive (sensitivity < 0.1).

3.3 Haemodynamic waveforms of CV model

Figure 3 shows the elastance and corresponding pressure plots of right and left heart. The elastance varies from their respective minimum diastolic value to their respective maximum end systolic value and vice versa from early diastolic relaxation to minimum end diastolic value in one cardiac cycle based on cosine function and the model predicted results are compared with the experimental results reported in Senzaki et al. (1996).

Figure 3 Elastance and pressure waveforms of heart: (a) left heart and (b) right heart

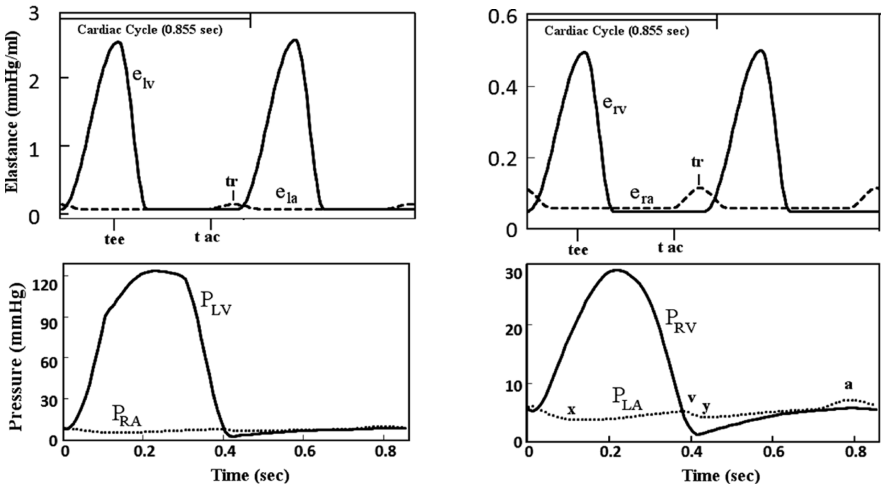

(a) (b)

The intra-arterial pressure has three positive waves called *a*, *c* and *v* and three negative waves namely *x*, *x*1 and *y* as shown in Figure 4 (Li, 2004; Guyton and Hall, 2006; Seeley et al., 2008). 'a' wave occurs during atrial systole, during which the phase pressure sharply raises to its maximum. The first negative '*x*' wave appears during the onset of atrial diastole. Because of the relaxation of atria, the pressure falls and the Atrioventricular (AV) valves close at the end of this wave. The *c* wave represents the isovolumetric contraction. The raise in the pressure is due to the closure of AV valve and the increase in the intraventricular pressure, which cause budging of AV valves into the atria. The *x*1 appears during ejection period because of the displacement of AV valves towards the ventricle. During atrial diastole, atrium is filled with venous return blood, which causes *v* wave. In the next phase, AV valves open and blood flows from atria to ventricle, which generates *y* wave. The ventricles pressure also follows the corresponding changes in pressure with respect to atrium pressure and is well matching with the experimental results reported by Senzaki et al. (1996). The ventricular volume plots (Figure 5) show ventricular filling (phase a; diastole), isovolumetric contraction (phase b), ejection (phase c) and isovolumetric relaxation (phase d) clearly as Li (2004), Guyton and Hall (2006), Akira et al. (2008) and Seeley et al. (2008) experimental results. The normal flow across tricuspid and mitral valve (Figure 5) shows characteristic pattern with initial rapid early flow (E-wave) and a smaller late atrial kick (A-wave) as reported in Greenberg et al. (2008). Vena cava and pulmonary vein flow pattern given by Akira et al. (2008) shows (Figure 6) *R* wave, which represents reverse flow, *S* wave represents systolic forward flow and *D* wave represents diastolic forward flow. Arterial pressure waveform has distinct Peak Systolic Pressure (PSP), Dichotic Notch (DN), Aortic Valve Open (AVO) and Aortic End-Diastolic Pressure (AEDP) phases.

Figure 4 Right atrial pressure

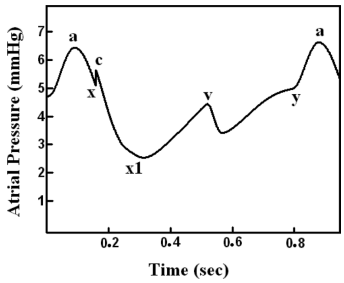

Figure 5 Heart volume and flow: (a) left heart volume, mitral and aortic flow and (b) right heart volume, tricuspid and pulmonary valve flow

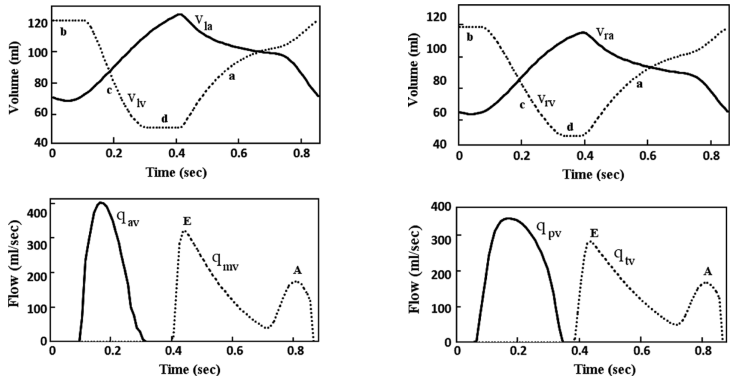

Figure 6 Systemic and pulmonary circulation flow patterns: (a) vena cava and artery flow and (b) pulmonary artery and vein flow

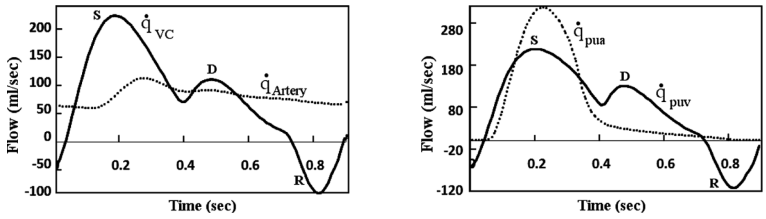

3.4 Dynamics of respiratory model

3.4.1 Lung mechanics

The time-varying pleural pressure (P_{pl}) is the driving force for the respiratory model. Respiratory dynamics are simulated for quite breathing starting with inspiration. For quite breathing, P_{pl} is negative, which is more negative in inspiration and less negative in expiration as shown in Figure 7(a). The corresponding changes in alveolar pressure are shown in Figure 7(b). The pressure in alveoli causes flow of air in and out of alveoli. During inspiration, because of negative *PA*, the atmospheric air enters the alveoli through

airways, lung recoil pressure increases simultaneously which compensates P_A changes and therefore ends inspiration phase. Pulmonary ventilation is a cyclic process, by which fresh air enters the lung and an equal volume of air is exhaled, which includes the anatomical parts where there is no gas exchange (dead space). The alveolar ventilation is different from the pulmonary ventilation. The alveolar ventilation indicates the volume of air, which is utilised for gaseous exchange. Figure 8 shows the pulmonary (dead space volume) and alveolar ventilation (alveoli volume). The model-simulated plots are matching with the experimental results reported in Barbini et al. (1994).

Figure 7 Pleural and alveoli pressure in quite breathing: (a) pleural pressure and (b) alveoli pressure

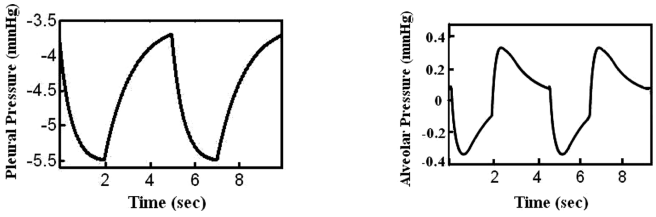

(a) (b)

Figure 8 Dead space and alveoli volume in quite breathing

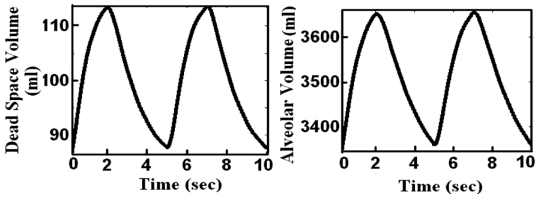

3.4.2 Gas exchange

Gas exchange occurs at the alveolar–capillary membrane owing to partial pressure gradient. The alveolar air is different from the inspired air. The alveolar air is partially replaced by the atmospheric air during each breath. Figure 9(a) shows partial pressure of O_2 and CO_2 in upper air way (Dead space) and Figure 9(b) in alveolar region (Hlastala, 1972; Guyton and Hall, 2006; Seeley et al., 2008). During inspiration through upper airway, O_2 rich atmospheric air enters alveolar region, which increases partial pressure of O_2 both in alveoli and in dead space and reduces CO_2 partial pressure and vice versa during expiration. The slope of the partial pressure plots for both O_2 and CO_2 in dead space is high (more changes in P_{O_2} and P_{CO_2}) compared with alveolar P_{O_2} and P_{CO_2} (less changes); this implies that alveolar P_{O_2} and P_{CO_2} is maintained nearly constant to facilitate continuous gas transfer between alveoli and capillary. The constant maintenance of P_{O_2} and P_{CO_2} is achieved by mixing of inhaled air with residual air at alveoli. The rate at which alveolar gas is renewed is slow in quite breathing. This is evident from different slopes of partial pressure graphs during inspiration and expiration. The slow renewal of alveolar air is important in preventing sudden changes in concentration of gases in the blood. The high-frequency variations in alveoli P_{O_2} and P_{CO_2} represent cardiac influences on gas exchange (cardiac frequency). The partial pressure of oxygen in the

atmosphere is nearly 159 mmHg and in the alveoli it is 106 mmHg (at the start of inspiration), because of the pressure gradient diffusion of oxygen from atmosphere to alveoli takes place. But, the partial pressure of oxygen in the pulmonary capillary is nearly 40 mmHg, which is less than P_{O_2} in alveoli (106 mmHg), which facilitates O_2 diffusion from alveoli into the blood. The reverse process occurs for CO_2. The results obtained from our model are having good agreement with the results reported in Lin and Cumming (1973) and Liu et al. (1998).

Figure 9 Partial pressure changes of O_2 and CO_2 in dead sapce and alveoli: (a) dead space (b) alveoli

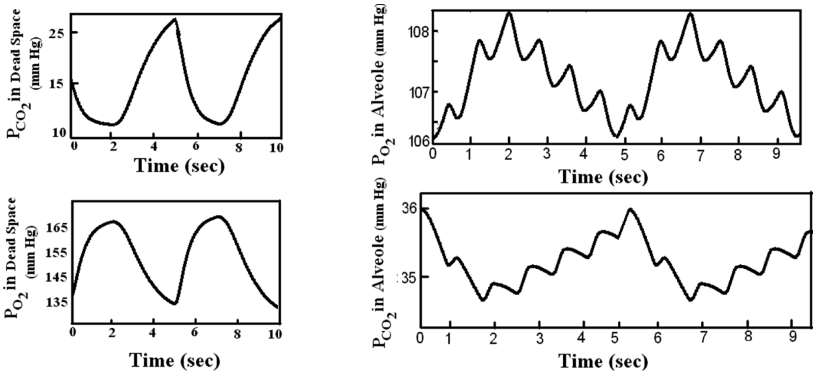

(a) (b)

3.5 CP interaction

Figure 10 shows the effect of respiratory-induced variation in aortic pressure (P_{ao}) for quite breathing. In quite breathing, P_{ao} is modulated with low-frequency respiratory rhythms. During inspiration because of high negative intrathoracic pressure, reduction in aortic pressure is observed. Negative P_{pl} increases the venous return, which results in reduced RV stroke volume. The reverse effect is observed in LV stoke volume, which leads to decrease in aortic flow and therefore slight decrease in aortic pressure in inspiration phase. The model-simulated haemodynamic variations are having good agreement with the experimental data reported in Robotham et al. (1979).

Figure 10 Arterial pressure phasic changes in quite breathing

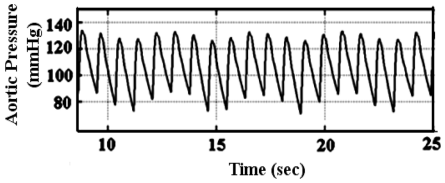

Valsalva Manoeuvre: Typical CP interaction is studied by VM. The VM is simulated by keeping P_{pl} as high positive pressure (30 mmHg for 15 s). The simulated arterial pressure in VM (Figure 11) exhibits four distinct phases as reported in Eduardo et al. (1991).

Figure 11 Aortic pressure in Valsalva manoeuvre condition

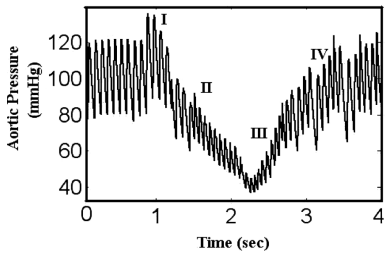

Phase I: During Phase I, the increase in arterial pressure is caused by the sudden elevation of intrathoracic pressure that expels blood contained in the cardiac and the pulmonary circulation into the peripheral circulation. In this phase, only heart rate is found to respond by a rapid increase, which is mediated by the quick withdrawal of vagal stimulus resulting from the unloading of the aortic and the CP receptors.

Phase II: Thereafter, during early Phase II, the reduction in venous return and the subsequent resultant decrease in cardiac output lead to a fall in arterial blood pressure. During this phase, heart rate keeps increasing to maintain arterial blood pressure. At the same time, sympathetic vasoconstriction and enhancement of cardiac contractility also begin to work against hypotension. However, because of the latency of sympathetic response, sympathetic activation is at a low level in this phase. During early Phase II, continual tachycardia, augmented sympathetic vasoconstriction and enhanced cardiac contractility function together to promote the active recovery of arterial blood pressure. In our model, sympathetic vasoconstriction and cardiac contractility are not implemented. Hence, in the late Phase II of simulated waveform, the recovery blood pressure is missing.

Phase III: During Phase III, the release of the strain results in a short-term sudden fall in arterial blood pressure, in response to which parasympathetic and sympathetic activations are further strengthened, evident in both the simulation and the experiments.

Phase IV: Thereafter, during Phase IV, the enhancement of vagal stimulus results in a negative overshoot in heart rate at the early stage, and the recovery of venous return along with the ANS-mediated regulation lead to a rapid increase in arterial blood pressure, again evident in the simulation.

4 Model limitations and extension

As in any physical model, our model also has some limitations.

1 the pulse wave propagation phenomenon is not addressed

2 ANS-mediated reflex activities such as CP reflex and chemoreflex are not considered

3 whole alveolar units are lumped as a single unit in respiratory model and upper airway bifurcations are not considered

4 it is a supine human model, so average P_{pl} is applied to all CV segments that lie in intrathoracic cavity

5 coronary circulation is omitted and also not possible to simulate regional disease

6 gravitational effect on haemodynamics is not included

7 the chest wall viscoelastance effect is not considered

8 gas transport at tissue level is not addressed.

However, this model has potential to address the above-mentioned limitations. This model also has the advantage of simulating CP diseases such as Mitral valve Stenosis (MS), mitral regurgitation, left heart failure, right heart failure, cardiac tamponade, pulsus paradoxus, asthma, sleep apnoea, emphysema and the influence of one system pathophysiology on the other system.

References

Akira, M., Noa, U., Atsuko, T., Kanako, M. and Mikio, M. (2008) 'The relationship between fetal inferior vena cava diameter pulse and flow velocity waveforms in normal and compromised pregnancies', *Early Human Development*, Vol. 84, No. 2, pp.129–135.

Anderson, J., Goplen, C., Murray, L., Seashore, K., Soundarrajan, M., Lokuta, A., Strang, K. and Chesler, N. (2009) 'Human respiratory mechanics demonstration model', *Advan. Physiol. Edu*., Vol. 33, pp.53–59.

Athanasiades, A., Ghorbel, F., Clark, J.W., Niranjan, S.C., Olansen, J.B., Zwichenberger, J.B. and Bidani, A. (2000) 'Energy analysis of a nonlinear model of the normal human lung', *J. Biol. Sys.*, Vol. 8, pp.115–139.

Barbini, P., Cevenini, G., Lutchen, K.R. and Ursino, M. (1994) 'Estimating respiratory mechanical parameters of ventilated patients: a critical study in the routine intensive-care unit', *Med. Biol. Eng. Comput*., Vol. 32, pp.153–160.

Benarroch, E.E., Opfer-Gehrking, T.L. and Low, P.A. (1991) 'Use of the photoplethysmographic technique to analyze the valsalva maneuver in normal man', *Muscle and Nerve*, Vol. 14, pp.1165–1172.

Beyar, R., Hausknecht, M.J., Halperin, H.R., Yin, F.C.P. and Weisfeldt, M.L. (1987) 'Interaction between cardiac chambers and thoracic pressure in intact circulation', *Am. J. Physiol*., Vol. 253 (*Heart Circ. Physiol.*, 22), pp.Hl240–H1252.

Burkhoff, D. and Tyberg, J.V. (1993) 'Why does pulmonary venous pressure rise after onset of LV dysfunction: a theoretical analysis', *Am. J. Physiol.*, Vol. 265 (*Heart Circ. Physiol*., 34), pp.H1819–H1828.

Cherniack, N.S. and Longobardo, G.S. (2006) 'Mathematical models of periodic breathing and their usefulness in understanding cardiovascular and respiratory disorders', *Exp Physiol*, Vol. 91, pp.295–305.

Chung, D.C., Niranjan, S.C., Clark Jr., J.W., Bidani, A., Johnston, W.E., Zwischenberger, J.B. and Traber, D.L. (1997) 'A dynamic model of ventricular interaction and pericardial influence', *Am. J. Physio*., Vol. 272 (*Heart Circ. Physio*., 41), pp.H2942–H2962.

De Boer, R.W., Karemaker, J.M. and Strackee, J. (1987) 'Hemodynamic fluctuations and baroreflex sensitivity in humans: a beat-to-beat model', *Am. J. Physiol.*, Vol. 253, No. 3, pp.H680–H689.

Fredberg, J.J. and Stamenovic, D. (1989) 'On the imperfect elasticity of lung tissue', *J. Appl. Physiol*., Vol. 67, pp.2408–2419.

Golden, J.F., Clark, J.W. and Stevens, P.M. (1973) 'Mathematical modeling of pulmonary airway dynamics', *IEEE Trans. Biomed. Eng*., Vol. 20, pp.397–404.

Greenberg, S.B., Shah, C.C. and Bhutta, S.T. (2008) 'Tricuspid valve magnetic resonance imaging phase contrast velocity-encoded flow quantification for follow up of tetralogy of fallot', *The International Journal of Cardiovascular Imaging (formerly Cardiac Imaging)*, Vol. 24, No. 8, pp.861–865.

Guyton, A.C. and Hall, J.E. (2006) *Textbook of Medical Physiology*, 11th ed., Elsevier Inc. Philadelphia, Pennsylvania, pp.471–506.

Hay, I., Rich, J., Ferber, P., Burkhoff, D. and Maurer, M.S. (2005) 'Role of impaired myocardial relaxation in the production of elevated left ventricular filling pressure', *Am. J. Physiol. Heart Circ. Physiol.*, Vol. 288, pp.1203–1208.

Hlastala, M.P. (1972) 'A model of fluctuating alveolar gas exchange during the respiratory cycle', *Respir. Physiol.*, Vol. 15, pp.214–232.

Hoit, B.D., Shao,Y., Gabel, M. and Walsh, R.A. (1993) 'Influence of pericardium on left atrial compliance and pulmonary venous flow', *Am. J. Physiol.*, Vol. 264 (*Heart Circ. Physiol*., 33), pp.H1781–H1787.

Jackson, A.C. and Milhorn, H.T. (1973) 'Digital computer simulation of respiratory mechanics', *Comput. Biomed. Res*., Vol. 6, pp.27–56.

Jonson, B., Beydon, L., Brauer, K., Mansson, C., Valind, S. and Grytzell, H. (1993) 'Mechanics of respiratory system in healthy anesthetized humans with emphasis on viscoelastic properties', *J. Appl. Physiol*., Vol. 75, pp.132–140.

Jung, E. and Lee, W. (2006) 'Lumped parameter models of Cardiovascular circulation in normal and arrhythmia cases', *J. Korean Math. Soc*., Vol. 43, No. 4, pp.885–897.

Li, J.K-J. (2004) *Dynamics of the Vascular System*, World Scientific Publishing Co. Pte. Ltd., Singapore, Vol. 1, pp.14–39.

Lin, K.H. and Cumming, G. (1973) 'A model of time-varying gas exchange in the human lung during a respiratory cycle at rest', *Respir. Physiol*., Vol. 17, pp.93–112.

Liu, C.H., Niranjan, S.C., Clark, J.W., San, K.Y., Zwischenberger, J.B. and Bidani, A. (1998) 'Airway mechanics, gas exchange, and blood flow in a nonlinear model of the normal human lung', *J. Appl. Physiol*., Vol. 84, pp.1447–1469.

Lu, K., Clark Jr., J.W., Ghorbel, F.H., Robertson, C.S., Ware, D.L., Zwischenberger, J.B. and Bidan, A. (2003) 'Cerebral autoregulation and gas exchange studied using a human cardiopulmonary model', *Am. J. Physiol. Heart Circ. Physiol.*, Vol. 286, pp.584–601.

Lu, K., Clark Jr., J.W., Ghorbel, F.H., Ware, D.L. and Bidani, A. (2001) 'A human cardiopulmonary system model applied to the analysis of the Valsalva maneuver', *Am. J. Physiol. Heart Circ. Physiol.*, Vol. 281, pp.2661–2679.

Luo, C., Ware, D.L., Zwischenberger, J.B. and Clark Jr., J.W. (2007) 'Using a human cardiopulmonary model to study and predict normal and diseased ventricular mechanics, septal interaction, and atrio-ventricular blood flow patterns', *J. Cardiovascular Engineering*, Vol. 7, pp.17–23.

Mukkamala, R. and Cohen, R.J. (2001) 'A forward model-based validation of cardiovascular system identification', *Am. J. Physiol. Heart Circ. Physiol.*, Vol. 281, pp.2714–2730.

Olansen, J.B., Clark, J.W., Khoury, D., Ghorbel, F.H. and Bidani, A. (2000) 'A closed-loop model of the canine cardiovascular system that includes ventricular interaction', *Comput. Biomed. Res.*, Vol. 33, pp.260–295.

Olender, M.F., Clark, J.W. and Stevens, P.M. (1976) 'Analog computer simulations of maximum expiratory flow limitation', *IEEE Trans. Biomed. Eng.*, Vol. 6, pp.445–452.

Robotham, J.L., Rabson, J., Permutt, S. and Brombergerbarnea, B. (1979) 'Left ventricular hemodynamics during respiration', *Am. J. Physiol*., Vol. 47, pp.1295–1303.

Rustagi, J.S. (1971) 'Mathematical models in medicine', *International Journal of Mathematical Education in Science and Technology*, Vol. 2 No. 4, pp.193–203.

Seeley, R.R., Stephens, T.D. and Tate, P. (2008) *Anatomy and Physiology*, McGraw-Hill College, ISBN-10: 0072965576.

Senzaki, H., Chen, C.H. and Kass, D. (1996) 'Single-beat estimation of end-diastolic pressure-volume relation in human: a new method with the potential non-invasive application', *Circulation*, Vol. 94, pp.2497–2506.

Shahin, M. and Maka, S. (2007) 'Linear state space model for long-term blood pressure regulation', *International Journal of Biomedical Engineering and Technology*, Vol. 1, No. 2, pp.190–203.

Sun, Y., Sjoberg, B.J., Ask, P., Loyd, D. and Wranne, B. (1995) 'Mathematical model that characterizes transmitral and pulmonary venous flow velocity patterns', *Am. J. Physiol.*, Vol. 268 (*Heart Circ. Physiol.*, 37), pp.H476–H489.

Sun, Y., Mazen, B., Rechard, J.L. and Salvatore, A.C. (1997) 'A comprehensive model for right-left heart interaction under the influence of pericardium and baroreflex', *Am. J. Physiol.*, Vol. 272, pp.H1499–H1515.

Glossary

Cardiovascular anatomical units considered in the model are abbreviated as follows. ven – venous, VC – vena cava, ra – right atrium, tv – tricuspid valve, rv – right ventricle, pv – pulmonary valve, pua – pulmonary artery, puc – pulmonary capillary, puv – pulmonary vein, la – left atrium, m – mitral valve, lv – left ventricle, av – aortic vave, ao – aorta, art – artery and cap – capillary.

B	Bernoulli's resistance (mmHg.s^2.ml^{-2})	E_s	Septum Elastance (mmHg/ml)
C	Compliance (ml/mmHg)	L	Inertance (mmHg.s^2.ml^{-1})
e	Time invariant elastance (mmHg/ml)	P_{it}	Intrathoracic pressure (mmHg)
E	Time varying elastance (mmHg/ml)	p_{pc}	Pericardial pressure (mmHg)
C_{Hb}	CO_2 binding sites on Hb(M)	V_{cw}	Chest wall volume (ml)
CO_{2_flux}	CO_2 flux at alveolar membrane (ml/min)	V_{cytox}	V_{max} for cytochrome oxidase in syst ISF (mole/min/g)
$Ct_{O_{2}\_ao}$	Concentration of O_2 in aorta (M)	V_D	Dead space volume (ml)
$Ct_{O_{2}\_\text{ISF}}$	Concentration of O_2 in ISF (M)	V_{O_2}	O_2 consumption (mole/min)
$Ct_{O_{2}\_\text{pua}}$	Concentration of O_2 in pua (M)	α_{O_2}	Solubility constant of O_2 in plasma (M/mmHg)
Cve	Compliance of lung tissue (ml/mmHg)	φ_{flux}	O_2, CO_2 flux between alveoli and puc (ml/sec)
DL_{O_2}	Diffusion capacity of O_2 (mlSTPD/s/mmHg)	P_{co}	Collapsible airways transmural ressure(mmHg)
$dS_{Hb_{O_2}\_ao}$	Derivative of saturation by O_2 in aorta (mmHg^1)	P_{cc}	Collapsible airway chamber pressure (mmHg)
$dS_{Hb_{O2}\_\text{pua}}$	Derivative of saturation by O_2 in pua (mmHg^1)	P_{H_2O}	Vapour pressure of water at body temp (mmHg)
H_{crit}	Hematocrit	P_l	Lung recoil pressure (mmHg)
K_{cytox}	Concentration of cytochrome Oxidase in systemic ISF (M)	P_{mouth}	Pressure at mouth (mmHg)

nH	Hill co-efficient	$P_{O_2\_ao}$	O_2 partial pressure in aorta (mmHg)
O_{2_flux}	O_2 flux (ml/sec)	$P_{O_2\text{-ISF}}$	O_2 partial pressure in interstitial fluid (mmHg)
$P_{50\_O_2}$	P_{50} of O_2 for Hb concentration (mmHg)	$P_{O_2\text{-pua}}$	O_2 partial pressure in pulmonary artery (mmHg)
P_A	Alveolar pressure (mmHg)	P_{pl}	Pleural pressure (mmHg)
Pao	External atm pressure (mmHg)	P_{STP}	STP pressure (mmHg)
$R_{\text{pao}_{O2}}$	Ratio of atmospheric P_{CO2} to $P_{CO2\text{-ao}}$ (mmHg)	Ru	Upper airways resistance (mmHg.sec/L)
$\dot{q}_{sm}$	Small airways flow (ml/sec)	RV	Residual volume (ml)
$\dot{q}_{co}$	Collapsible airways flow (ml/sec)	R_{ve}	Resistance of lung (mmHg.sec/L)
$\dot{q}_{up}$	Upper airways flow (ml/sec)	$S_{Hb_{O_2\_ao}}$	Aorta Hb_{O2} Saturation
$\dot{q}_{ve}$	Viscoelastic lung element flow (ml/sec)	$S_{Hb_{O_2\text{-ISF}}}$	Interstitial Hb_{O2} Saturation
R_c	Collapsible airways resistance (mmHg*sec/L)	$S_{Hb_{O_2\text{-pua}}}$	Saturation of O_2 in pua
R_s	Small airways resistance (mmHg. sec/L)	T_{body}	Body temperature (K)
v_c	Volume of collapsible airways (ml)	$P_{D_{O_2}}$	O_2 partial pressure in dead space (mmHg)
v_A	V_A Alveolar volume (ml)	$P_{A_{O2}}$	O_2 partial pressure in Alveoli (mmHg)
W_t	Body weight (Kg)	$P_{C_{O2}}$	O_2 partial pressure in collapsible airway (mmHg)

Appendix

Cardiovascular model

The haemodynamics of the CV model is completely defined by the following volume and flow equations. The volume change in any capacitive or elastance node should be equal to inflow minus outflow to achieve continuity.

Any elastance or capacitance node volume equation is written based on the general equation given here (Figure 12(a))

$$\mathrm{d}v/\mathrm{d}t = \dot{q}_{in} - \dot{q}_{\text{out}}$$

where Q_{in} is the inflow preload flow whereas Q_{out} is outflow from the corresponding node. For example, venous capacitance (C_{ven}) node and left ventricle elastance volume state equations are written as follows

$$\frac{\mathrm{d}v_{\mathrm{ven}}}{\mathrm{d}t} = \dot{q}_{\mathrm{cap}} - \dot{q}_{\mathrm{ven}}$$

$$\frac{\mathrm{d}v_{lv}}{\mathrm{d}t} = \dot{q}_{mv} - \dot{q}_{av}.$$

Figure 12 General elastance and inertance nodes in CVS model: (a) elastance (capacitance) and (b) inertance

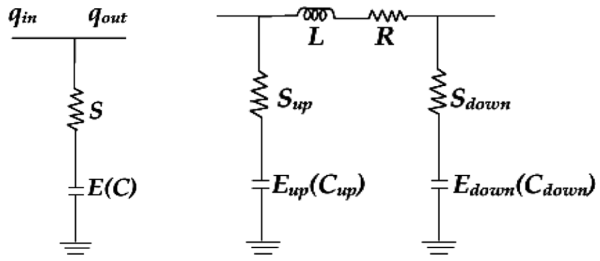

In similar way, all elastance/capacitance nodal equations (totally 12) are formulated.

The flow equations are formulated for every inertance node as shown in Figure 12(b).

$$\mathrm{d}\dot{q}/\mathrm{d}t = \left(p_{up} + S_{up}\,\mathrm{d}v_{up}/\mathrm{d}t - R\dot{q} - P_{\mathrm{down}} - S_{\mathrm{down}}\,\mathrm{d}v_{\mathrm{down}}/\mathrm{d}t \right) / L \quad .$$

Here, upstream and downstream parameters are considered. For example, venous inertance (L_{ven}) node and mitral valve inertance flow equations are written as follows

$$\frac{\mathrm{d}\dot{q}_{\mathrm{ven}}}{\mathrm{d}t} = \left(\frac{V_{\mathrm{ven}}}{C_{\mathrm{ven}}} + S_{\mathrm{ven}}\frac{\mathrm{d}v_{\mathrm{ven}}}{\mathrm{d}t} - R_{\mathrm{ven}}\dot{q}_{\mathrm{ven}} - \frac{V_{vc}}{C_{vc}} - S_{vc}\frac{\mathrm{d}v_{vc}}{\mathrm{d}t} \right) \Big/ L_{\mathrm{ven}}$$

$$\frac{\mathrm{d}\dot{q}_{mv}}{\mathrm{d}t} = \begin{cases} \left(e_{la}V_{la} - p_{lv} - R_{mv}\dot{q}_{mv} - b_{mv}\dot{q}_{mv}\left|\dot{q}_{mv}\right| - S_{lv}\frac{\mathrm{d}v_{lv}}{\mathrm{d}t} + S_{la}\frac{\mathrm{d}v_{la}}{\mathrm{d}t} \right) / L_{mv} & p_{la} > p_{lv} \\ 0 & \text{otherwise} \end{cases}$$

Respiratory model

In respiratory model, the mathematical formulae in gas exchange are given only for oxygen; formulae can be written for carbon dioxide by replacing corresponding parameters of CO_2

$$P_{\mathrm{I}} = A_{\mathrm{I}} \cdot \mathrm{e}^{k_I \cdot V_A} + B_{\mathrm{I}}$$

$$P_{\mathrm{CO}} = \begin{cases} A_c - B_c \cdot \left(\dfrac{V_c}{V_{c\max}} - 0.7 \right)^2 & V_c / V_{c\max} < 0.5 \\ A_c - B_c \cdot (0.5 - 0.7)^2 - B_{cp} \log\left(\dfrac{V_{c\max}}{V_c} - 0.999 \right) & V_c / V_{c\max} \geq 0.5 \end{cases}$$

$$P_A = P_{pl} + P_{ve} + P_l,\ P_{cc} = P_{pl} + P_{co},$$

$$P_{ve} = {V_{ve}}/{C_{ve}},\ P_s = P_{cc} + P_A$$

$$\dot{q}_{up} = \frac{P_{\mathrm{mouth}} - P_{cc}}{R_u + R_c},\ \dot{q}_{ve} = \frac{P_{ve}}{R_{ve}}$$

$$\dot{q}_{co} = \dot{q}_{up},\ \dot{q}_{sm} = \frac{P_s}{R_s}$$

$$\frac{\mathrm{d}v_c}{\mathrm{d}t} = \dot{q}_{co} - \dot{q}_{sm},\ \frac{\mathrm{d}v_A}{\mathrm{d}t} = \dot{q}_{sm} - \varphi_{\mathrm{flux}}$$

$$DL_{O_2} = 0.397 \sqrt{\frac{V_{\mathrm{puc}}}{V_{\mathrm{puc\_max}}}} + 0.0085^2 P_{O_2\_ao} - 0.0013^3 P_{O_2\_ao}^2 + \left(5.1e^{-7}\right)^4 P_{O_2\_ao}^3$$

$$DL_{co_2} = 16.67 \sqrt{\frac{V_{\mathrm{puc}}}{V_{\mathrm{puc\_max}}}}$$

$$O_{2\_\mathrm{flux}} = DL_{o2} \left(P_{A_{O2}} - P_{O_2\_ao} \right)$$

$$CO_{2\_\mathrm{flux}} = DL_{CO_2} \left(P_{A_{O2}} - P_{CO_2\_\mathrm{pua}} \right)$$

$$\varphi_{\mathrm{flux}} = \left(\frac{P_{\mathrm{STP}} T_{\mathrm{body}}}{\left(P_A + P_{\mathrm{STP}}\right) T_{\mathrm{body}}} \right) \left(O_{2\_\mathrm{flux}} + CO_{2\_\mathrm{flux}} \right)$$

$$S_{Hb_{O_2}\_ao} = \frac{\left(\dfrac{P_{O_2\_ao}}{P_{50\_O_2}} \right)^{nH}}{\left(\dfrac{P_{O_2\_ao}}{P_{50\_O_2}} \right)^{nH} + 1}$$

$$S_{Hb_{O_2}\_\mathrm{pua}} = \frac{\left(\dfrac{P_{O_2\_ao}}{P_{50\_O_2}} \right)^{nH}}{\left(\dfrac{P_{O_2\_ao}}{P_{50\_O_2}} \right)^{nH} + 1}$$

$$S_{Hb_{O_2\_\mathrm{ISF}}} = 100 S_{Hb_{O_2\_ao}}$$

$$Ct_{O_2\_ao} = \alpha_{O_2} P_{O_2\_ao} + C_{Hb} . S_{Hb_{O_2\_ao}} . H_{\mathrm{crit}}$$

$$Ct_{O_2\_\mathrm{pua}} = \alpha_{O_2} P_{O_2\_\mathrm{pua}} + C_{Hb} . S_{Hb_{O_2\_\mathrm{pua}}} . H_{\mathrm{crit}}$$

$$Ct_{O_2\_\mathrm{ISF}} = \alpha_{O_2} P_{CO_2\_ISF}$$

$$V_{O_2} = V_{\mathrm{cytox}} . W_t . \alpha_{O_2} . P_{O_2\_\mathrm{ISF}} \Big/ \left(K_{\mathrm{cytox}} + \left(\alpha_{O_2} . P_{O_2\_\mathrm{ISF}} \right) \right)$$

$$Pao_{O_2} = \left(Pao - P_{H_2O} \right) R_{\mathrm{pao}_{O2}}$$

$$\frac{P_{D_{O2}}}{\mathrm{d}t} = \begin{cases} \dot{q}_{up} Pao_{O_2} - \dot{q}_{co} P_{D_{O2}} \Big/ V_D & \dot{q}_{up} > 0 \\ \dot{q}_{up} P_{D_{O2}} - \dot{q}_{co} P_{C_{O2}} \Big/ V_D & \text{otherwise} \end{cases}$$

$$\frac{P_{A_{O2}}}{\mathrm{d}t} = \begin{cases} \dot{q}_{sm} . P_{C_{O2}} - P_{\mathrm{STP}} . T_{\mathrm{body}} . O_{2\_\mathrm{flux}} - P_{A_{O2}} \left(\dot{q}_{sm} - \varphi_{\mathrm{flux}} \right) \Big/ V_A & \dot{q}_{sm} > 0 \\ \dot{q}_{sm} . P_{A_{O2}} - P_{\mathrm{STP}} . T_{\mathrm{body}} . O_{2\_\mathrm{flux}} - P_{A_{O2}} \left(\dot{q}_{sm} - \varphi_{\mathrm{flux}} \right) \Big/ V_A & \text{otherwise} \end{cases}$$

$$\frac{P_{C_{O2}}}{\mathrm{d}t} = \begin{cases} \dot{q}_{co} P_{D_{O2}} - \dot{q}_{sm} P_{C_{O2}} - P_{C_{O2}} \left(\dot{q}_{co} - \dot{q}_{sm} \right) \Big/ V_c & \dot{q}_{sm} > 0 \\ \dot{q}_{co} P_{C_{O2}} - \dot{q}_{sm} P_{A_{O2}} - P_{C_{O2}} \left(\dot{q}_{co} - \dot{q}_{sm} \right) \Big/ V_c & \text{otherwise} \end{cases}$$

$$\frac{\mathrm{d}P_{O_2\_\mathrm{pua}}}{\mathrm{d}t} = \frac{F_{\mathrm{pua}} \left(Ct_{O_2\_ao} - Ct_{O_2\_\mathrm{pua}} \right) + DL_{O_2} \left(P_{A_{O2}} - P_{O_2\_\mathrm{pua}} \right)}{V_{\mathrm{pua}} \left(\alpha_{O_2} + H_{\mathrm{crit}} . C_{Hb} . \mathrm{d}S_{Hb_{O_2\_ao}} \right)}$$

$$\frac{\mathrm{d}P_{O_2\_\mathrm{ISF}}}{\mathrm{d}t} = \frac{PS.B_{wt} \left(P_{O_2\_\mathrm{pua}} - P_{O_2\_\mathrm{ISF}} \right)}{V_{\mathrm{ISF}}} - \frac{V_{O_2}}{\alpha_{O_2} . V_{\mathrm{ISF}}}$$

$$\frac{\mathrm{d}P_{O_2\_ao}}{\mathrm{d}t} = \frac{F_{ao} \left(Ct_{O_2\_\mathrm{pua}} - Ct_{O_2\_ao} \right) + PS\alpha_{o2} \left(P_{O_2\_\mathrm{ISF}} - P_{O_2\_ao} \right)}{V_{ao} \left(\alpha_{O_2} + H_{\mathrm{crit}} . C_{Hb} . dS_{Hb_{O2\_\mathrm{pua}}} \right)}$$